Solid-state NMR study of intercalated species in poly(e-caprolactone)/clay.

J. Hrobarikova, Jean-Louis Robert, C. Calberg, R. Jerome, J. Grandjean

Solid-State NMR Study of Intercalated Species in Poly(ε-caprolactone)/Clay Nanocomposites

J. Hrobarikova,1 J.-L. Robert3 C. Calberg,2 R. Jérôme,2 and J. Grandjean*1

University of Liege, Institute of Chemistry B6a, COSM

CERM, Sart Tilman, B-4000 Liege, Belgium,

ISTO, UMR 6113, CNRS-University of Orleans, 1A, rue de la Ferollerie, F-45071 Orleans Cedex 2, France

Abstract:

The structure and dynamics of surfactant and polymer chains in intercalated poly(ε-caprolactone)/clay nanocomposites are characterized by ^{31}P magic-angle spinning (MAS) and ^{13}C cross-polarization MAS NMR techniques. To obtain hybrid materials with the low polymer content required for this study, in situ intercalative polymerization was performed by adapting a published procedure. After nanocomposite formation, the chain motion of the surfactant is enhanced in the saponite-based materials but reduced in the Laponite ones. Compared to the starting clay, the trans conformer population of the surfactant hydrocarbon chain in the nanocomposite decreases for the saponite systems. Mobility of the polymer chain is higher in the nanocomposites than in the bulk phase. The charge of the modified saponite does not significantly influence chain mobility in the nanocomposites.

Introduction

Composites of polymers with smectite clay minerals[1] have received significant attention because of improvements in mechanical, thermal, and barrier properties that can result from synergistic effects of the polymers and the lamellar solid.[2-4] In particular, modified montmorillonite (MMT)-poly(ε-caprolactone) (PCL) nanocomposites (NANO) have been prepared recently.[5-11] These biodegradable materials have been characterized not only by macroscopic techniques such as X-ray diffraction, transmission electron microscopy, and thermal analysis[5-9,11] but also by X-ray photoelectron microscopy or Fourier transform infrared spectroscopy.[10] Microcomposites and intercalated nanocomposites have been obtained by direct melt blending of poly(ε-caprolactone) and sodium or organo-modified montmorillonites.[7] Exfoliated nanocomposites have been formed by a melt blending procedure[9] or in situ polymerization of ε-caprolactone with a modified clay[5,6] although an intercalated structure has been observed when the clay weight fraction is greater than 16%.[5] The effect of the clay dispersion within the polymer matrix on the composite properties has also been reported.[5,8,11]

Solid-state nuclear magnetic resonance (NMR) has emerged recently as a new tool to characterize clay/polymer nanocomposites.[12-21] NMR spectroscopy is known to be a powerful technique for probing the molecular structure, conformation, and dynamics of species at interfaces,[22,23] in complement to data from classical macroscopic methods. Natural montmorillonites are often used as raw materials for the preparation of nanocomposites, but the Fe(III) content of these aluminosilicates induces strong electron-nucleus dipolar interaction. The nuclear relaxation times of the intercalated species depend on the content and

distribution of iron species within the mineral, and the proton relaxation time has been proposed to characterize the clay dispersion within the polymer matrix.[12,13] While this approach has been successful for a few systems,[12,13,20] correlation with the clay distribution has been only observed in PCL systems obtained by the same preparation method.[21] Most NMR studies have used polymer nanocomposites formed with hectorite which is devoid of significant paramagnetic effects.[14-19]

In our previous NMR studies on modified clays,[22,23] we have used nonparamagnetic synthetic hectorite (Laponite) and saponites. These three-sheet clays result from 2:1 condensation, the octahedral layer being sandwiched between two tetrahedral layers. The clay platelets are negatively charged, as a result of cation isomorphous substitution either in the tetrahedral layer of saponites (Al(III) for Si(IV)) or in the octahedral layer of Laponite (Li(I) for Mg(II)). Exchangeable cations such as sodium occupy the interlamellar space to preserve electroneutrality.[1] We have exchanged Laponite[24] and saponites of a variable interlayer charge[25] with cationic surfactants. These materials which have been previously characterized[24,25] are used here to prepare PCL/clay nanocomposites.

The previous NMR investigations[12-21] of polymer/clay nanocomposites mainly deal with characterization of the bulk material containing a small amount of the mineral (typically 5%). As we are interested in the determination of the structure and dynamics of species near the clay surface, such systems are not appropriate, and we have prepared nanocomposites containing small amounts of PCL. Such materials allow one to study how the surfactant conformation and mobility are changed by the polymer adsorption and how the polymer motion is perturbed after intercalation in the nanocomposites. To our best knowledge, such NMR data have not been reported in the literature yet.

Experimental Section

Synthetic Na-saponites with a charge per half-unit cell in the 0.35-0.80 range (SAP0.35-SAP0.80) were prepared as described previously.[26] These phyllosilicates have been characterized by different methods.[26-28] Laponite RD (LAP) is a commercial synthetic hectorite (Laporte Industries Ltd.) with well-known properties. These clays were exchanged with the halides of hexadecyltrimethylammonium (HDTA), (2-hydroxyethyl)dimethylhexadecylammonium (HEDMHA), di(2-hydroxyethyl)methylhexadecylammonium (DHEMHA), or hexadecyltrimethylphosphonium (HDTP), as described previously.[24,25] The PCL-SAP and PCL-LAP nanocomposites were prepared by in situ polymerization catalyzed by dibutyltin dimethoxide, adapting a published procedure.[6] The polymerization was allowed to proceed at 55 °C for 48 h. Nanocomposites of low polymer content were obtained by varying the clay/monomer and monomer/dibutyl dimethoxide ratios. We have selected the nanocomposites prepared with the ratios 1/1 (w/w) and 10/1 (v/v) (method A) or 4/1-3/2 (w/w) and 7/2 (v/v) (method B), respectively. These materials were characterized by thermogravimetric analysis (Thermal Analyst 2100, TA Instrument; heating range of 20-800 °C at a heating rate of 10 °C/min, under N_2 flow) and X-ray diffraction (XRD) measurement (Powder Diffractometer Siemens D 5000; Cu Kα radiation λ= 1.54 Å, Ni-filter, 25 °C). The recovery of the nanocomposite polymer by clay extraction and the molecular weight determination were performed according to the literature.[6]

^{13}C cross-polarization (CP) magic-angle spinning (MAS) and ^{31}P MAS NMR spectra were recorded with 4 mm zirconia rotors spinning at 5 kHz on a Bruker Avance DSX 400WB

spectrometer (B_0 = 9.04 T) working at the Larmor frequency of 100.6 and 161.9 MHz, respectively. The CP NMR spectra were performed under high power proton decoupling (83 kHz) with a delay time of 4 s and a contact time of 2 ms. The time constants T_{CH} were determined from the plots of line intensity versus contact time in the CP MAS experiments. The conformer population of the surfactant alkyl chain in the nanocomposites was determined from these plots. The experiments (16 delays) were run with 3000 scans. The ^{13}C chemical shifts were calibrated on the terminal methyl group at 16.2 ppm relative to TMS. The ^{31}P longitudinal relaxation times in the laboratory frame $T_1(P)$ (15 delays, 100 scans) were measured according to a well-known procedure, using a 90° pulse of 4 μs. The ^{31}P chemical shift was referenced with respect to H_3PO_4 (85%).

Results and Discussion

The previous preparations of PCL/clay nanocomposites were based on low amounts, typically 5%, of dioctahedral aluminosilicate montmorillonites.[5-11] To avoid the structural paramagnetic ions of such phyllosilicates, we have used Laponite, a commercial synthetic hectorite, and synthetic saponites (trioctahedral magnesiosilicates) to prepare PCL nanocomposites with a rather high clay content, in the 50-70% range. Indeed, the aim of this study deals with the characterization of the structure and dynamics of species near the clay surface; hence high amounts of polymer overshadow the NMR signals of molecules at the organic-inorganic interface. The changes of the material composition and the structure and size of the clay platelets compared to those used previously[5-11] have required adaptation of a published procedure.[6] The first data deal with materials obtained by method A. In situ polymerization of ε-caprolactone with HDTA-LAP, HEDMHA-LAP, or DHEMHA-LAP provides nanocomposites giving a rather broad diffraction peak due to the small size of the Laponite platelets. The estimated basal d_{001} spacing of ca. 22 Å is higher than the value of 14.7 Å of the starting modified clays.[24,25] Values in the 30-33 Å range are observed for HDTP-SAP0.35-NANO, HDTP-SAP0.50-NANO, and HDTA-SAP0.50-NANO systems, indicating intercalation of poly(ε-caprolactone) chains between the clay layers.[5-7] More precisely, these materials contain a low percentage of oligo(ε-caprolactone) since the molecular weight is typically less than 1800. With such low polymer contents, the ^{13}C CP MAS NMR spectra of these nanocomposites mainly show the resonances of the surfactant whose signals are narrower in the nanocomposite than in the modified clay (Figure 1).

Higher mobility, reducing anisotropic interactions, or higher order shortening the frequency distribution may give rise to such behavior. Surfactant dynamics can be defined by ^{13}C CP experiments using different contact times. During the pulse sequence, the ^{13}C magnetization $M(t)$ increases exponentially with the time constant T_{CH} whereas the proton magnetization is governed by the relaxation in the rotating frame $T_{1\rho}(H)$, decreasing $M(t)$. The variation of the carbon magnetization is given by the equation

$$M(t) = M_0[\exp(-t/T_{1\rho}(H) - \exp(-t/T_{CH})]/\{1 - T_{CH}[T_{1\rho}(H)]^{-1}\} \quad (1)$$

where t is the contact time and M_0 is the equilibrium magnetization.

The usual assumptions in applying this equation[29] are fulfilled for our systems, and the three parameters M_0, T_{CH}, and $T_{1\rho}(H)$ can be obtained from the calculated curve. The cross-polarization is most efficient for static ^{13}C-^{1}H dipolar interactions and less mobile carbon

nuclei that exhibit smaller T_{CH} values. Analysis of the $T_{1\rho}(H)$ data is not so straightforward due to the interplay of molecular dynamics and the spin-diffusion process, and this parameter will not be considered further. The equilibrium magnetization M_0 provides quantitative information on the line intensity and in particular, the trans/gauche conformational ratio of the surfactant hydrocarbon chain has been determined from the intensity ratio of the methylene resonances at ca. 34 ppm (trans) and 32 ppm (gauche).

The dependence of the trans conformer population on the nature and charge of the modified clays has been discussed previously.[25] Recall that one single layer of surfactant is incorporated in Laponite with the long alkyl chain lying down on the clay surface. The gauche conformer is important, indicating chain flexibility. The modified saponites of low charge density show the same alkyl chain orientation within a bilayer arrangement of the surfactant cations. Isomorphous substitution in the tetrahedral layers of the saponites gives rise to stronger electrostatic interactions and more unfavorable interactions between the silicate layers and the nonpolar ammonium chains. This favors interchain interactions forming a bilayer structure and a higher population of the less flexible trans conformer. The mean surface area per cation modulates this conformer population which decreases for intermediate charge densities and increases again with the highest charge saponites, forming the so-called paraffin complex.[25] Intercalation of surfactants with long chain(s) in the dioctahedral montmorillonites results in a mainly trans conformation of the alkyl chains at room temperature.[30,31] In the Wyoming montmorillonites,[31] ca. 30% of the cation substitution occurs in the tetrahedral layer. Furthermore, the size of these natural clay platelets (≥1000 Å) is larger than that of Laponite (ca. 300 Å). Both effects can explain the high amount of gauche conformation in the modified Laponite.[24] On another hand, the T_{CH} values are 1 order of magnitude greater in the modified Laponite[24] than in the montmorillonite system,[30] supporting the greatest rigidity of the hydrocarbon chain in the latter system. With increasing temperature, conformation transformation takes place, leading to higher amounts of the more flexible gauche conformer.[24,30,31] The temperature dependence has been analyzed recently on montmorillonites exchanged with mono-, di-, tri-, and tetraalkylammonium cations of varying chain length.[31] At a certain length and number of chains, the molecules adopt an ordered state with a dominant trans conformation, due to increasing chain and packing density. With increasing temperature, this state is destroyed, leading to a more liquidlike behavior.[31]

The rather high flexibility of the hydrocarbon chain in the three modified-LAP materials seems to be preserved in the corresponding nanocomposites since the trans conformer population is not significantly perturbed (a 10% increase at the most). Compared to the values of the starting saponites, a significant decrease of the trans conformer population is observed after the nanocomposite formation. As noted, the time constant T_{CH} may provide a useful probe for chain dynamics. To keep constant the static dipolar interaction, relevant data are only obtained with the carbons bearing the same number of protons. As the surfactant polar headgroup does not significantly affect the signals of the methylene groups, we have only reported two typical sets of data (Table 1).

The surfactant-exchanged saponites are characterized by smaller T_{CH} values than those of the Laponite, in agreement with a stronger interaction of the headgroup with the tetrahedrally substituted saponites and with the higher content of the trans conformation of the surfactant alkyl chain.[25] Compared to the modified saponites, greater T_{CH} values of the HDTA hydrocarbon chain are observed in the nanocomposites (Table 1), indicating faster chain motion. This is consonant with the increase of the gauche conformation upon nanocomposite formation. With HDTA-LAP, HEDMHA-LAP, and DHEMHA-LAP in which the alkyl chain

mobility is high, a slowing down of this motion is detected in the hybrid materials (Table 1). A smaller increase of ca. 7-8 Å of the interlayer space in the Laponite materials instead of at least 10 Å in the saponite systems can explain these different observations. Insertion of at least one layer of oligomer in Laponite can account for the increase of the interlayer spacing of ca. 7-8 Å. For instance, the expected increase is 2.8 Å for a rigidly packed all-trans alkyl chain.[24] Since a surfactant monolayer is intercalated in Laponite, polymer formation induces favorable polymer-silicate interaction like in modified montmorillonite,[32] together with surfactant-polymer interactions, reducing mobility of the surfactant chain. The bilayer or pseudotrilayer arrangement of the organic cations intercalated in saponites, providing a greater gallery space advantageous for polymer insertion, could lead to oligomer adsorption at the center of the gallery causing more disorder and mobility enhancement of the surfactant chain. Cation substitution in the tetrahedral layers of the saponites should reduce polymer-silicate interactions, favoring the above process.

On another hand, the gauche conformation of the hydrocarbon chain (signal at 32 ppm) provides time constants T_{CH} greater than those of the trans conformer (signal at 34 ppm) in all the nanocomposites investigated, as expected from the higher rigidity of the last conformer (Table 1). Accordingly, the highest values are observed for the mobile terminal and polar head methyl groups. Similarly to the data with the modified clays,[25] the headgroup mobility of the LAP-NANOs decreases with the number of hydroxyethyl groups. For instance, the T_{CH} values of the NCH_3 groups are 443, 277, and 98.3 μs for the HDTA, HEDMHA, and DHEMHA systems, respectively. In the nanocomposites, this observation might result from the "steric" effect assumed with the modified clays[25] or from the involvement of the hydroxyethyl group(s) in the polymerization process.[6]

To support these results, the highly sensitive ^{31}P nucleus of HDTP samples provides a direct probe with which to compare the interaction between the positive end of the surfactant and the negatively charged clay. One single resonance is observed at ca. 25.5 ppm for the HDTP-exchanged clays and the corresponding nanocomposites. In the slow motion regime that applies here, a decrease in mobility leads to greater relaxation times in the laboratory frame $T_1(P)$. The interaction of the polar headgroup and the silicate surface is the weakest in the modified Laponite, and the shorter $T_1(P)$ value is observed. Accordingly, the stronger clay-surfactant interaction with the higher charge saponite gives rise to the greatest value (Table 2). The smaller relaxation times $T_1(P)$ observed for the two HDTP-SAP-NANOs and the greater value of HDTP-LAP-NANO compared to those of the precursor clays support the T_{CH} data showing a motional increase or decrease of the intercalated surfactant in the nanocomposites, respectively (Table 2).

The weak oligomer signals (Figure 1) are not useful for estimating polymer mobility, and more reliable data come from the nanocomposites prepared with method B which provides higher molecular weight polymers (Table 3). We have investigated the effect of the SAP0.40/monomer ratio and of the saponite charge on the polymer formation (Table 3).

The basal spacing values increase from 17.6 Å[25] to 20.7, 21.7, and 27.1 Å for the 8/2, 7/3, and 6/4 clay/monomer ratios, respectively. The last value shows intercalation of PCL between the clay platelets,[5-7] whereas the first two values indicate probably partial intercalation. As expected, the higher polymer content is observed for the lower saponite/monomer ratio. The ^{13}C CP MAS NMR spectra of the nanocomposites prepared with this ratio exhibit both useful HDTA and PCL signals, and a typical spectrum is shown in Figure 2.

Keeping constant the clay/monomer ratio, in situ polymerization was performed with modified saponites of increasing layer charge. The interplay between different interactions, that is, platelet-platelet interaction, polymer-silicate contacts, and polymer-surfactant alkyl chain interactions, is responsible for the nanocomposite formation. For instance, in their thermodynamic model for describing melt intercalation, Vaia and Giannelis have shown the importance of maximizing the number of favorable interactions between the polymer and the montmorillonite surface while minimizing the number of unfavorable interactions between the polar polymer and the nonpolar alkylammonium cations.[32] Several studies have suggested that the nature of the cationic surfactant is an important factor in the preparation of polymer/MMT nanocomposites. In particular, the surfactant loading has a great effect on the structure of organically modified clays and the structure and properties of the corresponding polymer/MMT nanocomposites.[33] Thus, it is generally considered that the higher basal spacing of the modified clay which can be obtained by increasing the length and the number of surfactant hydrocarbon chain(s) is advantageous for exfoliation in the synthesis of polymer nanocomposites.[31] However, better exfoliation in nylon-6 nanocomposites is shown with the surfactant bearing one single long hydrocarbon chain.[34] Thus, increasing the basal spacing of the organoclay does not necessarily lead to more exfoliation.

As the surfactant content of the HDTA-SAP samples is close to the cation exchange capacity (CEC), the surfactant loading increases with the clay charge. No clear effect is observed despite the differences of the gallery space and the extent of the cation isomorphous substitution of the starting saponites. Basal spacing values which fluctuate in the 27-37 Å range are consistent with the formation of intercalated nanocomposites (Table 3). The increase of the interlayer spacing is not simply related to the clay charge. One feature has to be noted: the experiment with SAP0.75 leads to a polymer yield of 25%, significantly higher than that obtained with the lower charge saponites (16-18%) (Table 3). Together with its higher cation exchange capacity, the platelet size of this clay, greater than that of the lower charge saponites,[27] favors polymer insertion between the mineral platelets. Better clay exfoliation is indeed observed with the increase of the clay platelet size.[35]

The assignments of the ^{13}C PCL signals are taken from the literature.[36] The carboxyl signal occurs near 175 ppm, whereas the C_6 peak at 66 ppm is partly resolved from the surfactant C_1 resonance (69 ppm) (Figure 2). The C_2 signal (34 ppm) is close to the chemical shift of the main methylene signal of the surfactant chain associated with the trans conformation. The 30-24 ppm region shows extra peaks compared to the spectrum of HDTA-SAP attributed to C_5 (30 ppm) and $C_{3,4}$ (27 ppm) of PCL. The trans conformer population of the surfactant alkyl chain decreases in all the investigated PCL-SAP-NANOs compared to its value in the precursor clay (Table 3). These results support the data of the nanocomposites obtained with method A.

The time constant values T_{CH} as a function of the used saponite/monomer ratio are summarized in Table 4. The HDTA values are intermediate between those of HDTA-SAP and the nanocomposite prepared by method A (Table 1). The formation of higher molecular weight polymers probably increases the rigidity of the surfactant chain compared to the previous systems (Table 1).

Decreasing the polymer content of the HDTA-SAP0.40-NANOs leads to lower T_{CH} values of the surfactant and the polymer nuclei. Such mobility reduction may result from a shorter interlayer space and a greater interaction with the clay surface. The small increase of the gallery space upon hybrid material formation (SAP/monomer ratios of 7/3 and 8/2) indicates

the formation not of intercalated nanocomposites but more probably of microcomposites. Therefore, the polymer chains could be mainly aggregated rather than isolated between the clay platelets. That is consistent with smaller T_{CH} values (see below). The other trends observed with these nanocomposites are similar to those reported for materials prepared with method A. As expected, the nonprotonated carboxyl carbon of PCL is characterized by a rather large T_{CH} value, due to a smaller ^{13}C-H dipolar interaction.

Method B has been used to prepare nanocomposites in order to obtain sufficiently intense PCL signals. The time constant values T_{CH} of the polymer obtained after extraction from the nanocomposite allow comparison of the macromolecular motion in the nanocomposite and in the bulk. Smaller values for the bulk polymer phase imply greater rigidity (Table 4), as a result of the interactions between the entangled chains. Intercalation of isolated polymer chains between the clay platelets reduces such interactions leading to higher mobility. A similar behavior has also been observed after surfactant intercalation in clays.[24] Finally, variation of the saponite charge between 0.75 and 0.35 charge per half-unit cell does not drastically perturb the dynamics of the surfactant and polymer in the nanocomposites. Typical values are shown in Table 5 for the highest and lowest charge saponites.

The lack of the clay surface effect is consistent with a polymer insertion at the center of the gallery space (not in contact with the silicate surface) where the interactions between the surfactant and polymer chains govern their dynamics, as assumed above to explain the different motional behaviors obtained for the nanocomposites prepared with modified saponites and Laponites.

Conclusions

Intercalated nanocomposites with a high clay content (50-70%) have been prepared by the in situ polymerization of ε-caprolactone in the presence of modified Laponite and saponites. Using the same experimental conditions, the highest polymer insertion has been found with the highest charge saponite. ^{13}C CP MAS experiments as a function of the contact time have been performed to determine the trans/gauche conformational ratio of the surfactant hydrocarbon chain and to characterize the surfactant and polymer mobility in the nanocomposites. Lower mobility of the surfactant hydrocarbon chain is observed after formation of the Laponite-based nanocomposites. When modified saponites are used to prepare the hybrid materials, the opposite effect is measured. The decrease of the trans conformer population in the surfactant hydrocarbon chain and the variation of the ^{31}P relaxation times of the intercalated phosphonium surfactant confirm the presence of higher mobility after nanocomposite formation. The segmental motion of poly(ε-caprolactone) is faster in the nanocomposites than in the bulk phase. No significant effect on the structure and dynamics of the nanocomposites was observed by varying the layer charge of the starting saponites, although the clay charge can affect the yield of the prepared nanocomposite. These results are explained in terms of different surroundings of the polymer chains in the bulk or intercalated in Laponite or saponites.

Acknowledgment

J.G. and R.J. are grateful to the FNRS (Bruxelles) for a grant to purchase the solid-state NMR spectrometer and to support this study. J.H. thanks the FNRS for a postdoctoral fellowship (2.4503.02). C. Boschini (Liege) is acknowledged for his technical assistance. The authors are very much indebted to "Belgian Science Policy" for financial support in the frame of the

"Interuniversity Attraction Poles Programme (PAI V/03) - Supramolecular Chemistry and Supramolecular Catalysis".

* To whom correspondence should be addressed. E-mail: J.Grandjean@ulg.ac.be.

†COSM.

‡CERM.

§CNRS-University of Orleans.

1. Theng, B. K. G. *The Chemistry of Clay-Organic Reactions*; J. Wiley: New York, 1974; Chapter 1.

2. Alexandre, M.; Dubois, P. *Mater. Sci. Eng., R.* **2000**, *98*, 1-63.

3. Gianellis, E. P.; Krishnamoorti, R.; Manias, E. *Adv. Polym. Sci.* **1999**, *138*, 107-147.

4. Fischer, H. *Mater. Sci. Eng.* **2003**, *C23*, 763-772

5. Tortora, M.; Vittoria, V.; Galli, G.; Ritrovati, S.; Chiellini, E. *Macromol. Mater. Eng.* **2002**, *287*, 243-249.

6. Lepoittevin, B.; Pantousier, N.; Devalckenaere, M.; Alexandre, M.; Kubies, D.; Calberg, C.; Jérôme, R.; Dubois, Ph. *Macromolecules* **2002**, *35*, 8385-8390.

7. Lepoittevin, B.; Devalckenaere, M.; Pantousier, N.; Alexandre, M.; Kubies, D.; Calberg, C.; Jérôme, R.; Dubois, Ph. *Polymer* **2002**, *43*, 4017-4023.

8. Gorrasi, G.; Tortora, M.; Vittoria, V.; Pollet, E.; Lepoittevin, B.; Alexandre, M.; Dubois, Ph. *Polymer* **2003**, *44*, 2271-2279.

9. Di, Y.; Iannace, S.; Di Maio, E.; Nicolais, L. *J. Polym. Sci., Part B*: *Polym. Phys.* **2003**, *41*, 670-678.

10. Viville, P.; Lazzaroni, R.; Pollet, E.; Alexandre, M.; Dubois, Ph.; Borcia, G.; Pireaux, J.-J. *Langmuir* **2003**, *19*, 9425-9433.

11. Pucciariello, R.; Villani, V.; Belviso, S.; Gorrasi, G.; Tortora, M.; Vittoria, V. *J. Polym. Sci., Part B*: *Polym. Phys.* **2004**, *42*, 1321-1332.

12. VanderHart, D. L.; Asano, A.; Gilman, J. W. *Chem. Mater.* **2001**, *13*, 3796-3809.

13. VanderHart, D. L.; Asano, A.; Gilman, J. W. *Macromolecules* **2001**, *34*, 3819-3822.[Full text - ACS] [ChemPort]

14. Yang, D.-K.; Zax, D. B. *J. Chem. Phys.* **1999**, *110*, 5325-5336. [ChemPort] [CrossRef]

15. Harris, D. J.; Bonagamba, T. J.; Schmidt-Rohr, K. *Macromolecules* **1999**, *32*, 6718-6724.[Full text - ACS] [ChemPort]

16. Hou, S. S.; Beyer, F. L.; Schmidt-Rohr, K. *Solid-State NMR* **2002**, *22*, 110-127. [ChemPort] [CrossRef]

17. Goddard, Y. A.; Vold, R. L.; Hoatson, G. L. *Macromolecules* **2003**, *36*, 1162-1169.[Full text - ACS] [ChemPort]

18. Hou, S.-S.; Bonagamba, T. J.; Beyer, F. L.; Madison, P. H.; Schmidt-Rohr, K. *Macromolecules* **2003**, *36*, 2769-2776.[Full text - ACS] [ChemPort]

19. Sahoo, K. S.; Kim, D. W.; Kumar, J.; Blumstein, A.; Cholli, A. L. *Macromolecules* **2003**, *36*, 2777-2784.[Full text - ACS] [ChemPort]

20. Bourbigot, S.; VanderHart, D. L.; Gilman, J. W.; Awad, W. H.; Davis, R. D.; Morgan, A. B.; Wilkie, C. A. *J. Polym. Sci., Part B*: *Polym. Phys.* **2003**, *41*, 3188-3213. [ChemPort] [CrossRef]

21. Calberg, C.; Jérôme, R.; Grandjean, J. *Langmuir* **2004**, *20*, 2039-2041.[Full text - ACS] [ChemPort]

22. Grandjean, J. *Annu. Rep. NMR Spectrosc.* **1998**, *35*, 216-260.

23. Grandjean, J. Nuclear magnetic resonance spectroscopy of molecules and ions at clay surfaces. In *Encyclopedia of Surface and Colloid Science*; Hubbard, A. T., Ed.; Marcel Dekker: New York, 2002; pp 3700-3712.

24. Kubies, D.; Jerome, R.; Grandjean, J. *Langmuir* **2002**, *18*, 6159-6163.[Full text - ACS] [ChemPort]

25. Müller, R.; Hrobarikova, J.; Calberg, C.; Jérôme, R.; Grandjean, J. *Langmuir* **2004**, *20*, 2982-2985.[Full text - ACS]

26. Bergaoui, L.; Lambert, J. F.; Frank, R.; Suquet, H.; Robert, J.-L. *J. Chem. Soc., Faraday Trans.* **1995**, *91*, 2229-2239. [ChemPort]

27. Michot, L. J.; Villiéras, F. *Clay Miner.* **2002**, *37*, 39-57. [ChemPort] [CrossRef]

28. Delevoye, L.; Robert, J.-L.; Grandjean, J. *Clay Miner.* **2003**, *38*, 63-69. [ChemPort]

29. Kolodziejski, W.; Klinowski, J. *Chem. Rev.* **2002**, *102*, 613-628.[Full text - ACS] [ChemPort] [Medline]

30. Wang, L.-Q.; Liu, J.; Exharos, J.; Flanigan, K. Y.; Bordia, R. *J. Phys. Chem. B* **2000**, *12*, 2810-2814.

31. Osman, M. A.; Ploetze, M.; Skrabal, P. *J. Phys. Chem. B* **2004**, *108*, 2580-2588.[Full text - ACS] [ChemPort]

32. Vaia, R. A.; Giannelis, E. P. *Macromolecules* **1997**, *30*, 8000-8009.[Full text - ACS] [ChemPort]

33. Zhao, Z.; Tang, T.; Qin, Y.; Huang, B. *Langmuir* **2003**, *19*, 7157-7159.[Full text - ACS] [ChemPort]

34. Fornes, T. D.; Hunter, D. L.; Paul, D. R. *Macromolecules* **2004**, *37*, 1793-1798.[Full text - ACS] [ChemPort]

35. Maiti, P.; Yamada, K.; Okamoto, M.; Ueda, K.; Okamoto, K. *Chem. Mater.* **2002**, *14*, 4654-4661.[Full text - ACS] [ChemPort]

36. Kaji, H.; Horii, F. *Macromolecules* **1997**, *30*, 5791-5798.[Full text - ACS] [ChemPort]

Figures

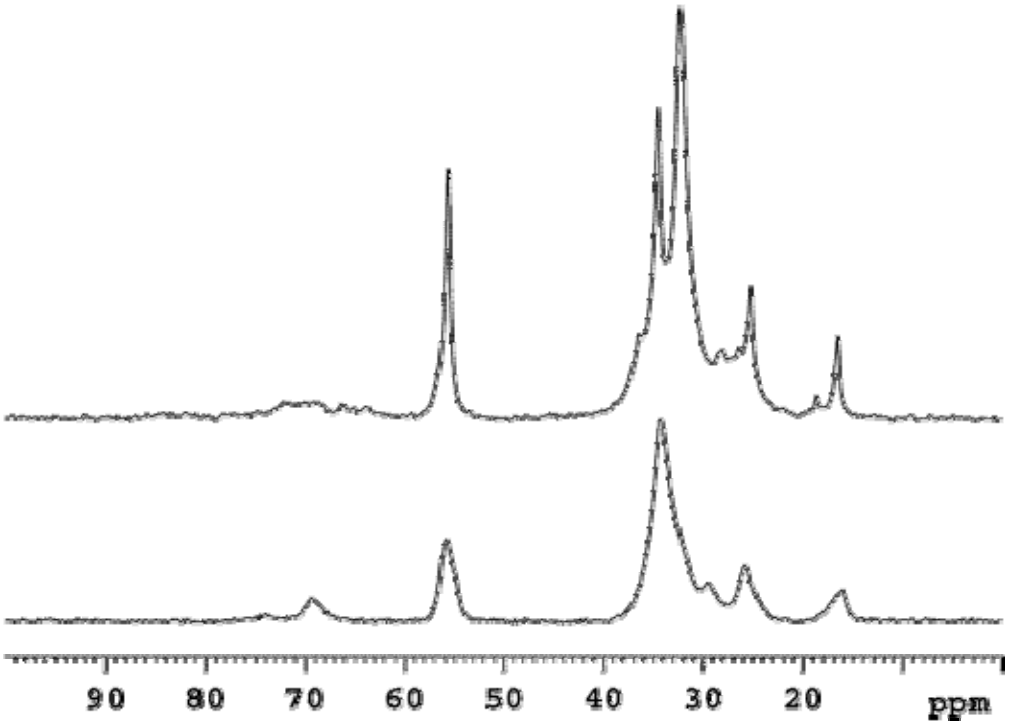

Figure 1 Typical ^{13}CP MAS NMR spectra of a modified saponite (bottom) and the corresponding nanocomposite (top) (method A).

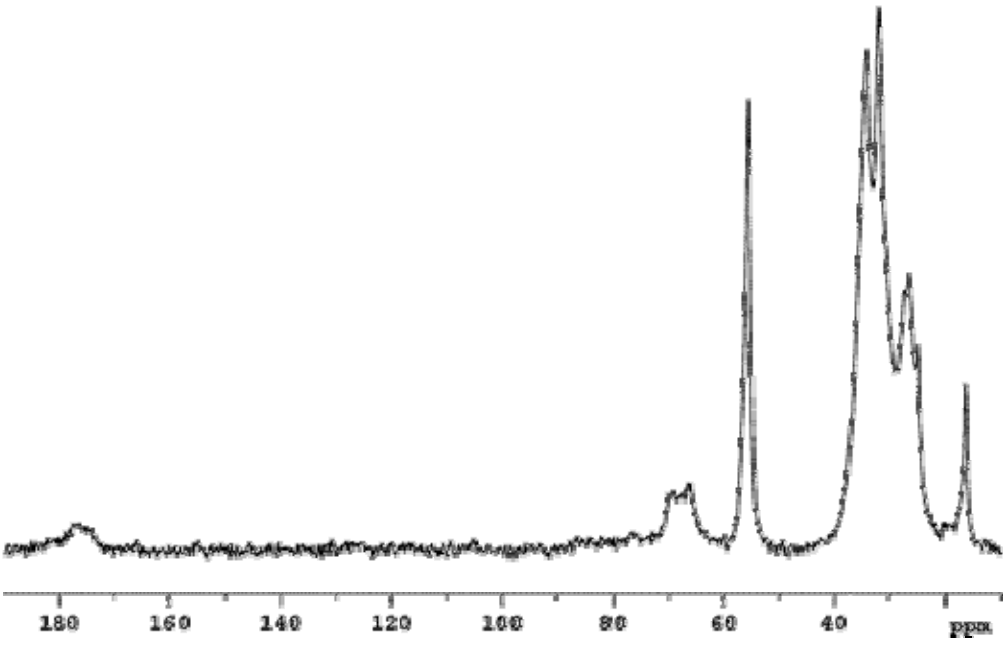

Figure 2 ^{13}C CP MAS NMR spectrum of the HDTA-SAP0.35 nanocomposite with a polymer content of 16% (method B).

Tables

Table 1. Time Constants T_{CH} (μs) of the HDTA Nuclei in Two Typical HDTA-Exchanged Clays and the Corresponding PCL Nanocomposites (Method A)

nucleus	T_{CH} (μs) SAP0.50	T_{CH} (μs) SAP0.50-NANO	T_{CH} (μs) LAP	T_{CH} (μs) LAP-NANO
C_{16}	409	2300	485	147
C_3	62.5	179	75.1	47.6
$C_{4\text{-}14}$(g)	n.d.	553	n.d.	68.1
$C_{4\text{-}14}$(t)	62.6	149	79.6	43.4
NCH_3	604	1066	796	443
C_1	41.9	104	48.1	38.9

Table 2. ^{31}P Spin-Lattice Relaxation Times in the Laboratory Frame T_1 (s) of Three HDTP-Modified Clays and the Corresponding PCL Nanocomposites (Method A)

sample	$T_1(P)$ MC	$T_1(P)$ NANO
HDTP-LAP	1.04	2.30
HDTP-SAP0.35	3.35	2.98
HDTP-SAP0.50	4.50	3.17

Table 3. Main Characteristics of the HDTA-SAP-PCL Nanocomposites Prepared with Method B

SAP/monomer (w/w)	d_{001} (Å)	trans conformer (%)[a] (used modified clay)[b]	polymer content (%)	M_n	M_w/M_n
8/2-SAP0.40	20.7	44 (70)	5	n.d.	n.d.
7/3-SAP0.40	21.7	47 (70)	11	3300	1.97
6/4-SAP0.40	27.1	61 (70)	17	3500	1.23
6/4-SAP0.75	36.8	45 (51)	25	4500	1.66
6/4-SAP0.60	32.7	20 (31)	16	5300	2.98
6/4-SAP0.50	34.9	51 (57)	18	3200	1.28
6/4-SAP0.35	30.3	38 (75)	16	3900	1.03

[a] The intensity of the PCL C_6 signal has been deduced from the signal at 34 ppm in order to account for the PCL C_2 signal occurring at the same position.[b] Reference 25.

Table 4. Time Constant Values T_{CH} of the HDTA-SAP0.40-PCL Nanocomposites Prepared with Method B as a Function of the SAP/Monomer Ratio

signal	T_{CH} (μs) 6/4	T_{CH} (μs) 7/3	T_{CH} (μs) 8/2
C_{16}	519	435	581
$C_{3,15}$	139	106	83.6
$C_{3,4}$-PCL	141 (74.1)[a]	n.d.	n.d.
C_5-PCL	n.d. (71.2)[a]	n.d.	n.d.
$C_{4\text{-}14}$, g	201	124	172
C_2-PCL; $C_{4\text{-}14}$, t	93.7 (78.1)[a]	97.8	84.7
NCH_3	1037	954	863
C_6-PCL	80.1 (69.8)[a]	73.0	59.1
C_1	63.4	61.6	54.7

[a] Values of the polymer after extraction from the nanocomposite.

Table 5. Time Constant Values T_{CH} of the HDTA-SAP-PCL Nanocomposites Prepared with Method B as a Function of the Saponite Charge

signal	T_{CH} (μs) SAP0.75	T_{CH} (μs) SAP0.35
C_{16}	740	512
$C_{3,15}$	92.5	91.3
$C_{3,4}$-PCL	87.5	88.3
$C_{4\text{-}14}$, g	146	142
C_2-PCL, $C_{4\text{-}14}$, t	92.5	84.7
NCH_3	709	798
C_6-PCL	59.5	65.8
C_1	49.6	60.9